



**POLITECNICO
DI TORINO**

THESIS FOR THE DEGREE OF MASTER OF SCIENCE IN PETROLEUM AND MINING ENGINEERING

SINGLE PHASE FLOW SIMULATION AT PORE SCALE

Porous Media Characterization Using 2D Single Phase Flow Simulation and
Sensitivity Analysis of The Minimum Thickness in 3D simulation

SUPERVISOR: PROF. DARIO VIBERTI
CO-SUPERVISOR: ENG. FILIPPO PANINI

BY: MUHAMMAD ABDELMAWGOUD EISSA MELEIGY
November 2020

Acknowledgements

Prophet, Muhammad, may Allah bless him and grant him peace, said,

"Allah does not thank the person who does not thank people."

First, I would like to express my gratitude to my supervisor Professor Dario Viberti, for his valuable insights, and for giving me this opportunity to learn a valuable and new concept for me.

Then, I am appreciative to my co-supervisor Mr. Filippo Panini for his help, support, and guidance in every step in this thesis.

I would like also to thank Mr. Mario Bello who gave me the opportunity to studying this Mater.

Last, I would like to thank my parents for all their hands.

Contents

1	Introduction	0
2	Objective	1
3	Porous Media Characterization at Pore Scale	2
3.1	Introduction	2
3.2	Porous Media	3
3.2.1	Definition of Porous Media	3
3.2.2	Pore Structure	6
3.2.3	Pore Size Distribution	7
3.2.4	Representative Volume Size (REV)	8
3.3	Navier-Stokes Equations	10
3.3.1	An overview of Navier Stokes Equations	10
3.3.2	Conservation of Mass	13
3.3.3	Conservation of Momentum	13
3.3.4	Conservation of Energy	16
3.4	Darcy's Law	17
3.4.1	The history of Darcy's Law	17
3.4.2	Explanation of the experiment	19
3.5	Kozeny-Carman	21
3.5.1	The theory of Kozeny-Carman equation	21
3.5.2	Hydraulic Radius Models	22
3.5.3	Derivation of Kozeny-Carman equation	22
3.6	Tortuosity	24
3.6.1	The concept of tortuosity	24
3.6.2	Tortuosity of flow in porous media	25
3.7	Effective porosity	27
4	Case studies, methodology and discussion of results	28
4.1	Case studies	28
4.2	Methodology	30
4.2.1	Finite Volume Method (FVM)	30
4.2.2	OpenFoam	31
4.3	Results and discussion	37
4.3.1	Part 1: porous media characterization	37
4.3.2	Part 2: Sensitivity analysis of the effect of the thickness of the 3D model on the calculated permeability using 2D+ model	40
5	Conclusion	42
6	References	43

List of figures

Figure 2.1 A field containing regular periodic cells Y with period ℓ ; $\ell/L \ll 1$	3
Figure 2.2 representing the solution of equation (2.2) with a rapidly fluctuating coefficient:	5
Figure 2.3 Representation of representative elementary volume REV and Porosity.....	9
Figure 2.4 Comparison between Lagrangian and Eulerian methods based on the way of observation of the fluid motion	11
Figure 2.5 Copy from the original illustration of Darcy's experimental apparatus which published by himself in 1856. (From Les Fontaine Publiques de la Ville de Dijon, Atlas, Figure 3)	18
Figure 2.6 Darcy's actual data used in the experiment	18
Figure 2.7 Simplified view of Darcy's experimental apparatus.	19
Figure 3.1 2D binary image of Berea sandstone	28
Figure 3.2 2D binary image of Hostun sandstone.....	29
Figure 3.3 2D binary image of Oodis.....	29
Figure 3.4 Mesh and dual mesh in FVM (a, b) vertex-centered and (c, d) cell-centered. The control volumes are the grey-colored areas	30
Figure 3.5 .stl file created using MATLAB for the original .jpg file for the rock image	32
Figure 3.6 a created background mesh done by blockMesh utility in OpenFOAM	33
Figure 3.7 the final mesh created by snappyHexMesh utility in the pore space only.....	33
Figure 3.8 A zoom on the non-interconnected pore space in Hostun rock image	34
Figure 3.9 The resulted mesh showing the effect of the effective porosity.....	34
Figure 3.10 velocity in x-direction results using simpleFoam solver	35
Figure 3.11 the MATLAB code used in permeability and tortuosity calculations.....	36
Figure 3.12 X-Direction velocity values resulting from the simulation of the three rock samples (a) Berea, (b) Hostun and (c) Oodis.....	38
Figure 3.13 Pressure values resulting from the simulation of the three rock samples (a) Berea, (b) Hostun and (c) Oodis.....	39
Figure 3.14 The velocity values in Z-direction for the 2D+ model showing a gradually change in the values	41
Figure 3.15 2D+ results of the sensitivity analysis of the thickness influence on the permeability values	41

1 Introduction

One of the most critical aspects in petroleum industry is to properly identify the host rock properties and the fluid characterization. The system of the rock and the fluids is called porous medium, and it can be defined as a multiphase system characterized by the occurrence of a solid matrix and a void “pore” space, both phases are distributed all over the domain. The different phases, one or more fluid phases occupying the pore space and a solid phase which is forming the grains of the matrix, they are separated from each other by definite interfaces.

One of those characterization is permeability which is considered as the ability of the rock to let fluids to pass through, based on the result of permeability determination, it will judge the reservoir will be able to deliver the hydrocarbon or not, however the determination of it starts long time ago with Henry Darcy, 1856.

To enhance accuracy porous media characterization, Digital Rock Physics has developed, the advances in both geophysical imaging (thin sections) and geological modeling will growth the knowledge about reservoir geology difficulties, which will enable to achieve optimum reserve calculations and determination of the economics of the development of the prospects.

With the advancing in computers and its invasion in all divisions, the direct numerical simulation is now widely used in petroleum industry, one of the applications of it is to simulate the fluid flow at pore scale which is considered as a microscale.

Navier-Stokes Equations in fluid mechanics are a set of a partial differential equation that describes the flow of incompressible fluids, In 1821 a French engineer named Claude-Louis Navier presented the element of viscosity for the more realistic and more difficult problem of viscous fluids. During the middle of the 19th century, a British scientist Sir George Gabriel Stokes enhanced this work, by completing the solutions were obtained only for the case of simple two-dimensional flows.

2 Objective

The objective of this work is divided into two main parts

The first part is to simulate a 2D single phase fluid flow at pore scale using different rock images to characterize those rocks by calculating the permeability and tortuosity

The second part of this work is to make sensitivity analysis to investigate the influence of the dimension of the third dimension on the calculated permeability results.

3 Porous Media Characterization at Pore Scale

3.1 Introduction

Porous media characterization on the microscopic level which means pore level is done for the purpose of understanding, simulating, and controlling the behavior and the properties of the macroscopic medium.

The terminology 'macroscopic' is an obvious concept and it usually refers to one or more set of samples of the medium on which some tests are performed in the lab.

As the transport properties of network modeling has shown that a cubic network of 15 x 15 x 15 mm, was adequately enormous to foresee similar conduct as bigger organizations, this might be taken as a sign of what establishes the base size of a homogeneous perceptible framework regarding nodes, representing pore bodies.

When alluding to macroscopic properties estimated in the lab it is likewise inferred that the sample utilized was 'homogeneous', i.e., if the sample were separated into at least two pieces, every one of which is as yet plainly visible, each piece would show a similar estimation of the originally visible property as the first (unbroken) sample.

As the sample might be almost homogeneous concerning one property (for example the porosity) than another property (for example the permeability), a genuinely homogeneous sample of a permeable medium is needed to be homogeneous as for all the properties which are identified with the pore structure.

Homogeneity In network modeling is ensured by disseminating the diverse pore sizes of a given probability density function (pdf) over a uniform structure of the network in the space so that there is a similar probability for every node of the network to be appointed a specific pore size, autonomously of the position of the node in the network. Accordingly, the pore sizes at any node are autonomous of one another, i.e., there is no spatial structure of pore sizes distribution.

The homogeneity characterized thusly is an exceptionally uncommon instance of a lot more extensive class of 'homogeneity' in the stochastic feeling of the word which allows a spatial structure of the property and specifies just ergodicity and stationarity of the property, inferring the equivalent pdf of all acknowledge of the property and a similar mean estimation of the property determined any point in the medium.

As the size of examination expands, it is generally found that spatial structure turns out to be significant and homogeneity in the tight, lab sense does not exist even roughly.

It is commonly understood that it is conceivable to demonstrate porous media transport properties with no reference to pore geometry, and simply utilize an enormous number of customizable boundaries in the model that do not have any actual importance.

3.2 Porous Media

3.2.1 Definition of Porous Media

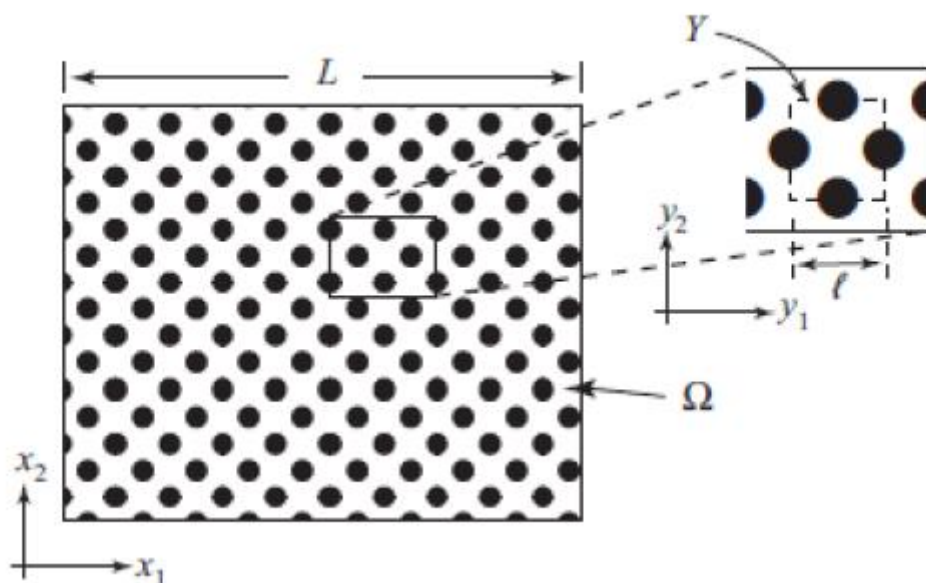


Figure 3.1 A field containing regular periodic cells Y with period ℓ ; $\ell/L \ll 1$.

A porous medium can be defined as a multiphase system characterized by the occurrence of a solid matrix and a void “pore” space, both phases are distributed all over the domain. The different phases, one or more fluid phases occupying the pore space and a solid phase which is forming the grains of the matrix, they are separated from each other by definite interfaces.

To understand how a domain which has those features can influence transport phenomena, it is considered here a simplified porous medium (see figure 2.1) of size L with a synthetic well-sorted periodic pattern, with l representing the period ($\varepsilon = l/L$ is the ratio). The stationary diffusive transport ($u(x)$) in X direction is modeled by the Laplace differential equation¹:

$$\frac{d}{dx} \left[a(x) \frac{du(x)}{dx} \right] = 0, \quad 0 \leq x \leq L \quad 3.1$$

subject to the boundary conditions

$$u(0) = 0, \quad u(L) = 1 \quad 3.2$$

Because of the periodic pattern, $a(x)$ is a variable coefficient of diffusion. assume $L = 1$, therefore $l = \varepsilon$, and $a(x)$ is a periodic function, with period ε

$$a(x) = \frac{1}{1+2 \sin^2 \frac{\pi x}{\varepsilon}} \quad 3.3$$

¹ the Laplace transform is an integral transform used to switch a function from the time domain to the s -domain. The Laplace transform can be used in some cases to solve linear differential equations with given initial conditions.

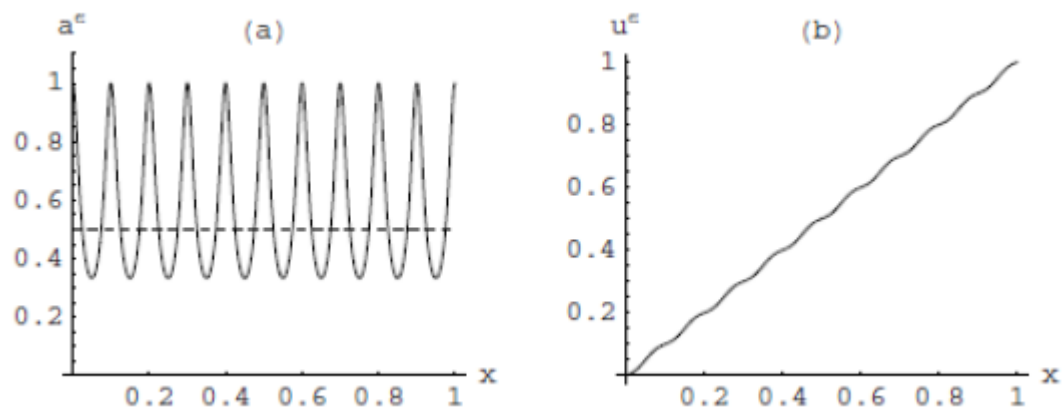


Figure 3.2 representing the solution of equation (2.2) with a rapidly fluctuating coefficient:
 (a) a plot showing a as in equation (2.3), with $\epsilon = 0.1$, where the dashed line indicates the effective coefficient aH ;
 (b) the solution (2.4) for $u(x)$.

For $\epsilon = 0.1$, the coefficient is plotted in figure (2.2), where we observe 'rapid' fluctuations (small period) with a large amplitude (due to the difference of the coefficient value in the solid grains and in the single fluid phase occupying the void space). The exact solution of the problem represented by (2.1) and (2.2) for $1/\epsilon$ an integer, is

$$u(x) = \frac{\int_0^x \frac{dx}{a(x)}}{\int_0^1 \frac{dx}{a(x)}} = \frac{4\pi x - \epsilon \sin \frac{2\pi x}{\epsilon}}{4\pi - \epsilon \sin \frac{2\pi}{\epsilon}} = x - \frac{\epsilon}{4\pi} \sin \frac{2\pi x}{\epsilon} \quad 3.4$$

The solution is plotted in figure (2.2) for $\epsilon = 0.1$. The function (2.4) consists of two parts: a slowly varying part (linear) with rapidly fluctuating, small amplitude ripples superposed on top. Thus, the magnitude of the disturbance in the solution, caused by the fluctuating coefficient $a(x)$, is controlled not by the coefficient's amplitude, but by its period (ϵ), which is small. The other quantity of interest is the flux q of the property $u(x)$

$$q = -a(x) \frac{du(x)}{dx} = - \frac{u(1)-u(0)}{\int_0^1 \frac{dx}{a(x)}} \quad 3.5$$

where we can identify the harmonic mean $a_H = L / \int_0^L \frac{dx}{a(x)}$ with $L = 1$ size of the macroscopic domain, leading to the expression

$$q = a_H \frac{u(0)-u(L)}{L} = \frac{1}{2} \quad 3.6$$

where the value of a_H is plotted as the dashed line in fig. (2.2).

The conclusions we obtain from the example above are that:

1. integration on a large-scale domain (as in the case of the local differential Laplace equation) produces a distribution of the integrated argument upon which the effect of the local microscopic behavior of the properties is negligible since it is of the order $O(\varepsilon)$.
2. the microscopic configuration effects are lumped in coefficients (such as a_H) created in the process of averaging (integrating).

3.2.2 Pore Structure

The term "pore structure" means various things. On the bottom level of information, it can be interpreted as the "porosity" ϕ , i.e., the fraction of the volume of the pores within the porous material. The foundation of considering that pore structure is the porosity is the perception that other properties for example permeability can be predicted from the porosity. For a rock volume, V , comprising

of a total volume of solid (s), and fluid (f), can be represented as $V = V_s + V_f$, porosity ϕ can be denoted as the volume of void spaces per the total volume of the sample in other words it can be represented as $\phi = 1 - (V_s / V)$, which is one minus the solid volume fraction.

Porosity is that feature of a porous medium that involves the routes and the volume accessible for fluid flow and carriage as well as for storage and maintaining of water.

3.2.3 Pore Size Distribution

On a more sophisticated level of information pore structure can be interpreted as a characteristic pore size. More generally pore structure is usually identified with what is called pore size distribution. Pore size distribution is a poorly defined quantity because it depends on the measuring method used in its identification. The most common procedure used for the identification of a pore size distribution consists of the measurement of some physical properties in rely on another physical quantities under the operator control and fluctuated in the experiment.

As an example, in mercury porosimeter, the volume of mercury entering the sample is measured as a function of the pressure applied on the mercury, in vapor sorption, the volume of absorbed gas which is measured as a function of the pressure applied on the gas, the volume of displaced miscible liquid is measured as a function of the volume of injected liquid displaced into the sample in a miscible displacement experiment, etc.

Pore size distribution can be defined as the density function which gives the distribution of pore volume by a characteristic pore size. However, the volume parameter is generally measured directly, but the characteristic pore size is always estimated from some physical parameters that is measured in terms of the arbitrary model of pore structure.

Because of the complexities of pore geometry, the characteristic pore size is not always reflecting the actual characteristic of the pore volume which it has been assigned to.

3.2.4 Representative Volume Size (REV)

Orienting our attention to the fluid/s, which is contained in the pore space, and trying to characterize the phenomena associated with them, e.g. mass transport, motion etc., some difficulties are faced. First, the fluid concept itself requires more elaboration. Fluids are composed of a lot of molecules (facing the existence of a structure of the sub molecular) that move around, colliding with: a) each other and b) with the walls of the container which they are placed in.

Applying theories of classical mechanics, a fully description of a system of molecules can be given for example, their momenta, their initial positions in space also their future positions can be predicted. Although the simplicity of that approach, it is too difficult to solve the problem of the motion of even three molecules (supposing that all the forces are well known, which is also uncertainties).

With the usage of high-speed computers, most of the body problems can be solved, in practice, numerically. It is still impossible to specify the motion of molecules of about 1^{23} in one-gram mole of any gas. Additionally, due to the huge number of molecules, their momenta and their initial positions cannot be determined correctly.

Consider a domain occupied by the porous medium and G a mathematical point inside it. Consider a volume ΔV_i (which has the shape of a sphere) which is larger than a single grain or pore, for which G is the centroid. For this volume we may determine the ratio:

$$n_i \equiv n_i(\Delta V_i) = (\Delta V_u)_i / \Delta V_i \quad 3.7$$

Where $(\Delta V_u)_i$, is the volume of pore space within ΔV_i . iterating the same procedure, a series of values $n_i(\Delta V_i)$, $i = 1,2,3, \dots$ can be obtained by decreasing the size of ΔV_i around G as a centroid: $\Delta V_1 > \Delta V_2 > \Delta V_3 \dots$.

For large values of $(\Delta V_u)_i$, the ratio n_i may be subjected to gradual changes as ΔV_i , is reduced, particularly when the examined domain is heterogeneous. Lower than a particular value of ΔV_i , relying on the distance of G from boundaries of the domain, these fluctuations tend to decay, leaving little amplitude fluctuations that are because of the random distribution of pore sizes about G. Nevertheless, below a certain value ΔV , huge fluctuations in the ratio n_i may be observed. This occurs as the dimensions of ΔV_i is getting closer to those of a single pore.

Finally, as $\Delta V_i \rightarrow 0$, convergence on the mathematical point G, n_i will get either one or zero, relying on whether G is inside the solid matrix or inside a pore space of the domain. Figure 2. 3 shows the relationship between n_i and ΔV_i .

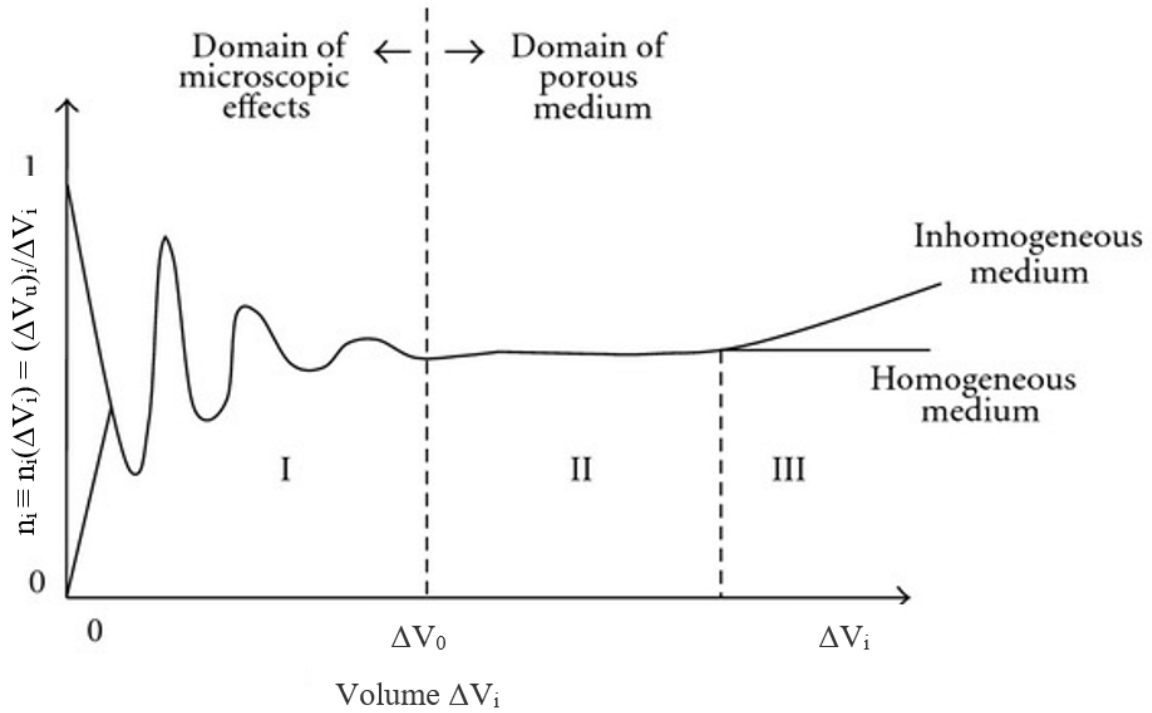


Figure 3.3 Representation of representative elementary volume REV and Porosity.

Technological breakthrough and increasing of facilities availability for high-resolution 3D imaging, for example x-ray microtomography (μ CT), led to a significant increase in the 3D visual data related the porous media features at pore scale. Quantification of pore scale features is fundamental in enhancing the understanding of the core basis of macroscopic fluid transport behavior.

With the aim to achieve the maximum spatial resolution, for example $10 \mu\text{m}$, and enough x-ray penetration through the sample, the samples which are used for μ CT imaging are usually small (3–7 mm as inner diameter) [Wildenschild et al., 2002; Altman et al., 2005].

Additionally, only a central sub-volume of the original 3D image is used for the quantitative analysis to eliminate the wall effects that affect the packing of the matrix and the distributions of the fluids. Therefore, quantitative measurements are usually made on a 3D region of $<100 \text{ mm}^3$ [Clausnitzer and Hopmans, 1999; Culligan et al., 2004; Al-Raoush and Willson, 2005a; Brusseau et al., 2008; Costanza-Robinson et al., 2008; Narter and Brusseau, 2010; Porter et al., 2010]. [3] As shown in Figure 2.3 for porosity and REV, at

small spatial scales (region I) some fluctuations in porosity, coupled with pore scale heterogeneity, are observed. The measurements of porosity which made at that scale can only be regarded as unreliable results of the measurement scale.

For homogeneous porous media, a minimum representative elementary volume (REV) can be defined as the boundary of region II; measurements of porosity which made at that scale are independent on the scale and precisely represent a larger system.

For heterogeneous porous media, REV can conceptually be obtained at scales between the false fluctuations of region I and the macroscopic heterogeneity of region III, although the presence of region II for real heterogeneous systems may be difficult to delineate with confidence [Zhang et al., 2000; Baveye et al., 2002].

3.3 Navier-Stokes Equations

3.3.1 An overview of Navier Stokes Equations

The movement and the transport of fluids in a physical domain is controlled by several properties. For the aim of understanding the fluid flow behavior and introducing a mathematical model, those properties must be defined accurately as to provide a development between the physical and the numerical domain.

The main properties that must be taken into consideration concurrently when performing a fluid flow examination are velocity, temperature, pressure, viscosity, and density. Turbulence, multiphase flow, combustion, mass transport, etc., in compliance with the physical phenomena are diversify extensively and can be classified into transport, thermodynamic, kinematic, and other properties.

Cases of thermo-fluid directed by governing equations are based on conservation laws. During dynamic and/or thermal interactions, the Navier Stokes equations (NSE) are the commonly used mathematical model to analyze changes in those properties. The equations are adaptable to the substance of the issue and are expressed on the basis of the concepts of conservation of momentum, energy and mass.

- Continuity Equation represents the Conservation of Mass
- Newton's Second Law represents Conservation of Momentum

- First Law of Thermodynamics or Energy Equation represents Conservation of Energy

However, some authors specify the term Navier-Stokes equations only for the conservation of momentum, some of them still use all the conservation equations of the physical properties. Concerning the conditions of fluid flow, NSE are reprioritized to provide corrective solutions in which the complexity of the problem changes for which it either increases or decreases. For example, to have a numerical model of turbulence according to Reynolds number which has pre-calculated needs an adequate turbulent model to be implemented to obtain trusted results.

Even though the movement of fluid is an investigative topic for our knowledge, the progress of mathematical models began at the end of 19th century after the industrial revolution. The preliminary appropriate explanation of the viscous fluid movement had been indicated in the paper “Principia” by Sir Isaac Newton (1687) in which the fluids dynamic

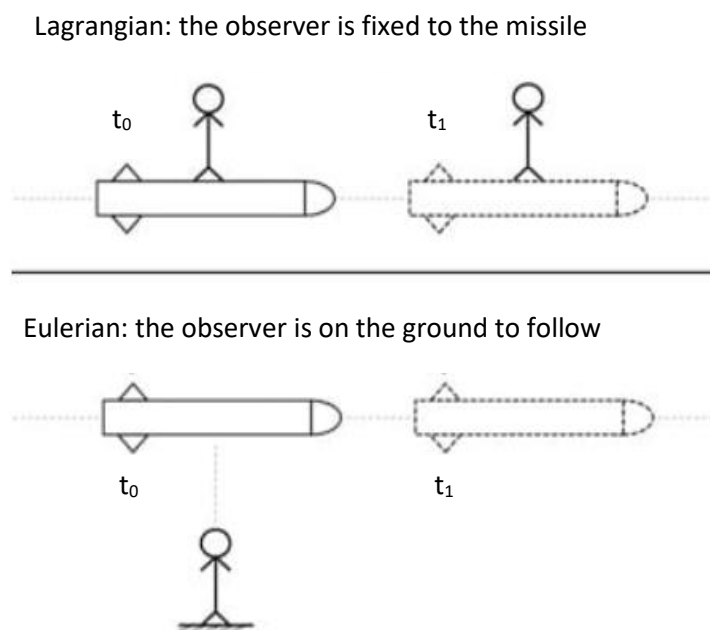


Figure 3.4 Comparison between Lagrangian and Eulerian methods based on the way of observation of the fluid motion

behavior under constant viscosity was explored. Later, Daniel Bernoulli (1738) and Leonhard Euler (1755) consequently derived the equation of inviscid flow which is now expressed as Euler’s inviscid equations. Although Claude-Louis Navier (1827), Augustin-Louis Cauchy (1828), Siméon Denis Poisson (1829), and Adhémar St.Venant (1843) had

performed studies to investigate the mathematical model for a fluid flow, they had neglected the viscous force.

By adding Newtonian viscous terms, Sir George Stokes in 1845 had derived the equation of motion for a viscous flow, in this manner the Navier-Stokes Equations had been developed to their final form which has been used to create numerical solutions for fluid flow from the time when.

To generate an appropriate mathematical model, the observation method of fluid flow on the basis of kinematic properties is a fundamental matter. The movement of fluid can be examined with either Lagrangian or Eulerian methods.

Lagrangian method describes fluid motion based on observing a fluid particle that is large enough to identify properties. There are millions of individual particles must be analyzed through the path between the initial coordinates at initial time t_0 and coordinates of the same particle at time t_1 , which is almost impossible to follow.

On the other hand, in the Eulerian method, no specific particle across the path is followed; as an alternative, the velocity field as a function of time and position is analyzed. The missile example (Figure 2.4) exactly fits to highlight those methods.

The formulation of Lagrangian equation of motion is continually time dependent. Let a , b , and c are the initial coordinates of a particle; and x , y , and z are its coordinates at time t .

So, the motion description based on Lagrangian is the following:

$$x = x(a, b, c, t) \quad y = y(a, b, c, t) \quad z = z(a, b, c, t) \quad 3.8$$

On the other hand, in the formulation of Eulerian method, the components of velocity at the point (x, y, z) are u , v and w while t is the time. In this method the unknowns are the velocity components u , v and w , which in corresponding are functions of the independent variables space (x, y, z) and time t . The formulation of motion using the concept of Eulerian method for any value of t is:

$$u = u(x, y, z, t) \quad v = v(x, y, z, t) \quad w = w(x, y, z, t) \quad 3.9$$

In the Eulerian system in which fluid motion is described, the equations of conservation are stated as Continuity Equation for mass, Navier-Stokes Equations for momentum and Energy Equation for the first law of Thermodynamics. The equations are all considered at the same time to investigate fluid and flow fields.

3.3.2 Conservation of Mass

The mass in the control volume can be neither be created nor destroyed. The conservation of mass states that the mass flow difference throughout the system between inlet and outlet is zero:

$$\frac{D\rho}{Dt} + \rho(\nabla \cdot \vec{V}) = 0 \quad 3.10$$

Where ρ is the Density while V is the velocity.

The fluid is assumed to be incompressible and the density is constant, then the continuity equation can be simplified as following:

$$\frac{D\rho}{Dt} = 0 \rightarrow \nabla \cdot \vec{V} = \frac{\partial u}{\partial x} + \frac{\partial v}{\partial y} + \frac{\partial w}{\partial z} = 0 \quad 3.11$$

3.3.3 Conservation of Momentum

In a control volume the momentum is kept constant, which involves the conservation of momentum that we call ‘The Navier-Stokes Equations’. The expression is set up based on the description of Newton’s Second Law of Motion:

$$F = m \times a \quad 3.12$$

Where F is the force applied to any particle, a is the acceleration, and m is the mass. In case of a fluid, it is appropriate to express that equation in terms of the volume of the particle as the following:

$$\rho \frac{DV}{Dt} = f = f_{body} + f_{surface} \quad 3.13$$

Where f is the force applied on the fluid particle per unit volume, and f_{body} is the force exerted on the whole mass of fluid particles as follows:

$$f_{body} = \rho g \quad 3.14$$

where g is the gravitational acceleration. The external forces which are applied through the fluid particles surface, $f_{surface}$ is expressed using pressure and viscous forces as:

$$\tau_{ij} = -p\delta_{ij} + \mu \left(\frac{\partial u_i}{\partial x_j} + \frac{\partial u_j}{\partial x_i} \right) + \delta_{ij}\lambda \nabla \cdot V \quad 3.15$$

Therefore, Newton's equation of motion can be specified as follows:

$$\rho \frac{DV}{Dt} = \rho g + \nabla \cdot \tau_{ij} \quad 3.16$$

Substitution of equation (2.16) into (2.15) results in the Navier-Stokes equations of Newtonian viscous fluid in one equation:

$$\underbrace{\rho \frac{DV}{Dt}}_I = \underbrace{\rho g}_{II} - \underbrace{\nabla p}_{III} + \underbrace{\frac{\partial}{\partial x_i} \left[\mu \left(\frac{\partial v_i}{\partial x_j} + \frac{\partial v_j}{\partial x_i} \right) + \delta_{ij} \lambda \nabla \cdot V \right]}_{IV} \quad 3.17$$

I: Momentum convection

II: Mass force

III: Surface force

IV: Viscous force

Where p is the static pressure and ρg is the gravitational force. Equation 2.17 is suitable for fluid and flow fields which are both compressible and transient.

If case of the density of the fluid is constant, the equations can be significantly simplified in which $\nabla \cdot V = 0$ and the viscosity coefficient μ is assumed to be constant in equation (2.17).

Thus, the Navier-Stokes equations for a three-dimensional incompressible flow can be expressed as follows:

$$\rho \frac{DV}{Dt} = \rho g - \nabla p + \mu \nabla^2 V \quad 3.18$$

For each dimension as the velocity is $V(u, v, w)$:

$$\rho \left(\frac{\partial u}{\partial t} + u \frac{\partial u}{\partial x} + v \frac{\partial u}{\partial y} + w \frac{\partial u}{\partial z} \right) = \rho g_x - \frac{\partial p}{\partial x} + \mu \left(\frac{\partial^2 u}{\partial x^2} + \frac{\partial^2 u}{\partial y^2} + \frac{\partial^2 u}{\partial z^2} \right) \quad 3.19$$

$$\rho \left(\frac{\partial v}{\partial t} + u \frac{\partial v}{\partial x} + v \frac{\partial v}{\partial y} + w \frac{\partial v}{\partial z} \right) = \rho g_y - \frac{\partial p}{\partial y} + \mu \left(\frac{\partial^2 v}{\partial x^2} + \frac{\partial^2 v}{\partial y^2} + \frac{\partial^2 v}{\partial z^2} \right) \quad 3.20$$

$$\rho \left(\frac{\partial w}{\partial t} + u \frac{\partial w}{\partial x} + v \frac{\partial w}{\partial y} + w \frac{\partial w}{\partial z} \right) = \rho g_z - \frac{\partial p}{\partial z} + \mu \left(\frac{\partial^2 w}{\partial x^2} + \frac{\partial^2 w}{\partial y^2} + \frac{\partial^2 w}{\partial z^2} \right) \quad 3.21$$

The unknowns in the equation are p , u , v and w , where a solution is brought by the implementation of both continuity equation and boundary conditions. Moreover, the energy

equation must be taken into consideration if any thermal interface is available in the problem.

3.3.4 Conservation of Energy

Conservation of Energy is expressed in the first law of thermodynamics which states that the sum of the work and heat added to the system will result in the increase of the total energy of the system:

$$dE_t = dQ + dW \quad 3.22$$

where dQ is the heat added to the system, dW is the work done on the system, and dE_t is the total energy of the system.

The Navier-Stokes equations have a structure which is non-linear with numerous complexities and therefore it is too difficult to carry out an exact solution for those equations. Subsequently, different assumptions are required to bring the equations to a possible solution.

Using the mathematical model, it simply gives relations among parameters that are part of the whole process. Consequently, the solution of the Navier-Stokes equations can be achieved with either analytical or numerical methods.

The analytical method only compensates solutions in the case which non-linear and complex structures in the Navier-Stokes equations are overlooked within numerous assumptions. The analytical approach is only valid for simple/fundamental cases such as Couette flow, Poiseuille flow, etc.

On the other hand, almost every case in fluid dynamics includes non-linear and complex structures in the mathematical model which cannot be ignored. Therefore, the solutions of the Navier-Stokes equations are executed within several numerical methods, the constantly encountered of Ordinary Differential Equations (ODEs) and Partial Differential Equations (PDEs).

3.4 Darcy's Law

3.4.1 The history of Darcy's Law

Starting in 1856 Henry Darcy, a French hydraulic engineer interested in purifying water supplies using sand filters, with the assistance of Henry Bazin, issued four works that show various forms of an improved Pitot tube design. Even Though Henri Pitot had invented the device in 1732, its theoretical vulnerabilities, and design weaknesses had kept it little more than a scientific toy. Darcy conducted experiments to determine the flow rate of water through the filters, his conclusions have served as the basis for all modern analysis of ground water flow

Darcy's has improved instruments which provided precise and easy measurements of point velocity, which allowed improvements in open channel and hydraulics of pipe flow. His final design for the instrument tip is reflected today in all our modern instruments. A reproduction of Darcy's published 1858 design was completed and shown to work as reported.

Darcy's contribution to the development of the device equaled or surpassed Pitot's initial work, thus making it applicable to refer to the modern instrument as the "PitotDarcy tube"

A few career highlights¹:

- In 1828, Darcy was assigned to a deep well drilling project that found water for the city of Dijon, in France, but could not provide an adequate supply for the town. However, under his own initiative, Henry set out to provide a clean, dependable water supply to the city from more conventional spring water sources. That effort eventually produced a system that delivered 8 m³/ min from the Rosoir Spring through 12.7 km of covered aqueduct.

- In 1848 he became Chief Director for Water and Pavements, Paris. In Paris he carried out significant research on the flow and friction losses in pipes, which forms the basis for the Darcy-Weisbach equation for pipe flow.

- He retired to Dijon and, in 1855 and 1856, he conducted the column experiments that established Darcy's law for flow in sands.

¹ Freeze, R. Allen. "Henry Darcy and the Fountains of Dijon." *Ground Water* 32, no.1(1994): 23–30

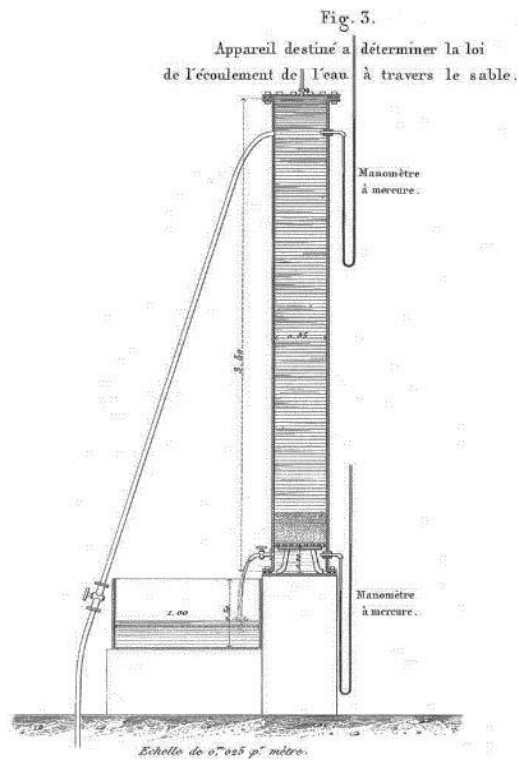


Figure 3.5 Copy from the original illustration of Darcy's experimental apparatus which published by himself in 1856. (From Les Fontaine Publiques de la Ville de Dijon, Atlas, Figure 3)

Figure 2.5 shows the original work of Mr. Henry Darcy. This consisted of a vertical iron pipe, 3.50 meters in length and 0.35 meters in diameter, both ends are flanged. Its height is 0.20 meters above the base of the column, a horizontal screen was placed which supported by an iron grillwork, a column rested upon it, a meter in length of loose sand.

Water could be introduced into the system by a pipe, which tapped into the column near the top, from the building water supply, and could be discharged through a valve from the open chamber near the bottom, and his results are illustrated in figure 2.6.

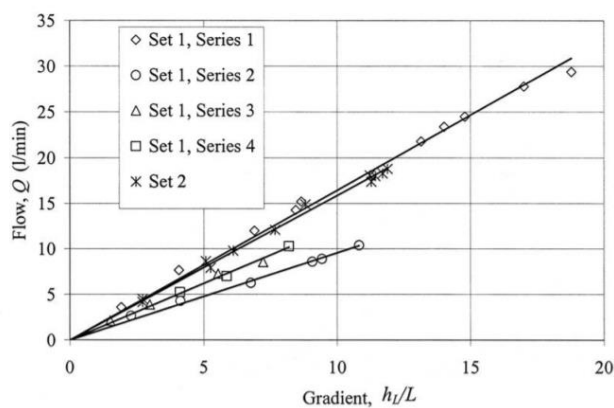


Figure 3.6 Darcy's actual data used in the experiment

3.4.2 Explanation of the experiment

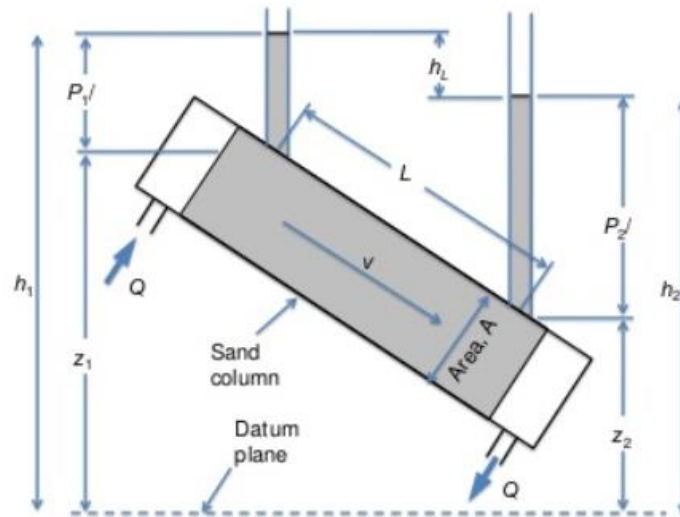


Figure 3.7 Simplified view of Darcy's experimental apparatus.

Where q is the volume flow rate of water downward through the cylindrical sand pack. The sand pack has a cross-sectional area A and a length L . h_1 is the height above a datum of water in a manometer which is located at the inlet face. h_2 is the height above a datum of water in a manometer located at the outlet face.

The following assumptions are implied in Darcy's experiment:

1. Single-phase flow (only water)
2. Vertical flow
3. Homogeneous porous medium (sand)
4. Single geometry
5. Non-reactive fluid (water)

Darcy concluded the following points:

- The volume flow rate of the fluid "water" is directly proportional to the difference of water level in the two manometers, i.e.: $q \propto h_1 - h_2$
- The volume flow rate of the fluid "water" is directly proportional to the cross-sectional area of the sand pack, i.e.: $q \propto A$

- The volume flow rate of the fluid “water” is directly proportional to the length of the sand pack, i.e.: $q \propto L$.

So, all the above relations can be written follows:

$$q = K \frac{A}{L} (h_1 - h_2) \quad 3.23$$

Where K is the proportional constant termed hydraulic conductivity which depends on the rock and fluid properties.

For the fluid effect:

- K is directly proportional to the fluid specific weight, i.e. $K \propto \gamma$
- And inversely proportional to the fluid viscosity, i.e. $K \propto \mu$

For the rock effect:

- K is directly proportional to the square of grain size, i.e.: $K \propto d^2$
- Inversely proportional to tortuosity, i.e.: $K \propto 1/\tau$
- And inversely proportional to the specific surface, i.e.: $K \propto 1/S_s$, Where $S_s = \text{Interstitial surface area/bulk volume}$.

Combining the above un-measurable rock properties into one property, which is called permeability, and denote it by k, we get:

$$q = k \frac{\gamma A}{\mu L} (h_1 - h_2) \quad 3.24$$

Since

$$q = vA \quad 3.25$$

Thus 2.24 can be written as the general Darcy form:

$$v = \frac{q}{A} = \frac{k \Delta p}{\mu \Delta L} \quad 3.26$$

Units: v : cm/s

q : cm³/s A : cm² k : Darcy

P: atm

L: cm

μ : cpoise

3.5 Kozeny-Carman

3.5.1 The theory of Kozeny-Carman equation

For permeability (k) determination, numerous equations have been theoretically, experimentally, and empirically developed (e.g., Slichter, 1899; Van Terzaghi, 1923; Krumbein and Monk, 1942; Wyllie and Rose, 1950; Loudon, 1952; Rose, 1957; Harr, 1962; Chilingar et al., 1963; Davis and De Wiest, 1966; Berg, 1970; Todd, 1980; De Marsily, 1986; Katz and Thompson, 1986; Johnson et al., 1987). Those equations are dependent, one way or another, on three fundamental equations: Darcy's equation (see section 2.4), Poiseuille's equation, and the Kozeny-Carman equation.

For a fluid with viscosity μ (in Poise) flowing through a number of capillary tubes n_c , each with capillary length L_c and capillary radius r_c (both in cm), where ΔP is in dyne/cm², the general form of the Poiseuille's equation for capillary flow is:

$$q = \frac{N_c \pi r_c^4 \Delta P}{8\mu L_c} \quad 3.27$$

Because the porosity in Poiseuille's model is given by $\phi = N_c(\pi r_c^4/4)L/L$ the permeability k can be expressed as

$$k = \phi r_c^2 / 8 \quad 3.28$$

Using the equations of Darcy 2.26 and Poiseuille 2.27, Kozeny (1927) derived an equation that was later modified by Carman (198) and was thus known as the Kozeny-Carman equation.

“In the theory proposed by Kozeny, the porous medium is treated as a bundle of capillary tubes of equal length, these tubes are not necessarily of circular cross-section, yet he does not take into account velocity components normal to the tubes' axes as a result of the diverging or converging nature of the flow in the tubes” Bear, Jacob -1972.

3.5.2 Hydraulic Radius Models

The concept of hydraulic radius R can be defined as the ratio between of cross-sectional area and the wetted perimeter and is often used in open channels and flow through pipes.

As an example, consider a circular pipe has a radius r , so the cross-sectional area will be πr^2 and the wetted perimeter is $2\pi r$, therefore the hydraulic radius $R = r/2$.

Hydraulic radius can be also defined as the ratio of volume of a channel filled with fluid to its wetted surface area. This definition combined with a conception of the porous medium as a network of channels that are interconnected with each other, leads to a relationship between R and the specific surface (M) defined by $R = \varphi/M$.

Where M is the specific surface of a porous material and is defined as the total interstitial surface area of the pores (A_s) per unit bulk volume (V_b) of the porous medium

$$M = A_s/V_b \quad 3.29$$

Thus, R represents an equivalent (or average) hydraulic radius of the complicated flow channels.

Returning to Poiseuille's equation for flow in a pipe, and replacing $2r$ by $4R$, we obtain:

$$V = -\frac{R^2}{2} \frac{\rho g \Delta P}{\mu L_c} \quad 3.30$$

3.5.3 Derivation of Kozeny-Carman equation

From the point of capillary tube bundle stated by Bear, Kozeny's model looks like the model of capillary tube, by using Navier-Stokes equations solving for all channels passing through a cross-sectional area which is normal to the flow in the porous medium, Kozeny obtains the equations for motion and permeability in the forms:

$$q = -(c_0 \varphi^3 / \mu M^2) grad p; \quad k = c_0 \varphi^3 / M^2 \quad 3.31$$

c_0 is a numerical coefficient which called Kozeny's constant; it depends on the geometrical form of each channel in the model.

($c_0 = 0.5$ for a circle, $= 0.662$ for a square, $= 0.597$ for an equilateral triangle and $c_0 = 0.667$ for a strip).

The equation of k in 2.31 is called Kozeny's equation, substituting the hydraulic radius $R = \varphi/M$, the k in 2.28 will be:

$$k = \varphi^3 / 2M^2 \quad 3.32$$

with expressing the specific surface regarding a unit volume of solid, instead of regarding a unit volume of porous medium (M , in 2.29), we obtain from (2.31):

$$k = c_0 [\varphi^3 / (1 - \varphi)^2] / M_s^2 \quad 3.33$$

In 1937 Carmen used that form of Kozeny's formula with $c_0 = \frac{1}{5}$:

$$k = [\varphi^3 / (1 - \varphi)^2] / 5M_s^2 \quad 3.34$$

The equation 2.34 is known as the Kozeny-Carman equation.

In this equation the porosity factor $f(\varphi)$ is stated as $\varphi^3 / (1 - \varphi)^2$. It can be possible to introduce a term representing the particle size by $d = 6/M$, thus 2.33 can be written as:

$$k = \frac{d_m^2}{180} \frac{\varphi^3}{(1 - \varphi)^2} \quad 3.35$$

After the introducing Kozeny's equation and the modification of Carmen; it's more convenient to mention its relationship with tortuosity τ (will be discussed in the next section), we obtain the following modified forms of 2.31 and 2.33:

$$k = c_0 \varphi^3 / \tau M^2 \quad \text{or} \quad k = c_0 [\varphi^3 / (1 - \varphi)^2] / \tau M_s^2 \quad 3.36$$

3.6 Tortuosity

3.6.1 The concept of tortuosity

One of the common characteristics of the transportation of any material through porous media, for instance fluid flow or electric current, is that the actual route which the transported material tracks is very complicated, or “tortuous” at the microscopic scale. The concept of tortuosity is often introduced in the framework of solving the termination problem for transport in porous media, i.e., in the derivation of the macroscopic transport equations concerning the averaged quantities individually.

A conventional method of determining tortuosity is to start with a simplified model of the porous medium, such as the capillary tube model, then generalize the outcomes for the more realistic porous media. This generalization may be done by presenting a further parameter which is supposed to regard the more complicated transport routes which have been neglected in the starting model, tortuosity can be used as that parameter. As any other physical parameter, tortuosity may be characterized in different ways.

Possibly the most perceptive and simple definition of tortuosity is that of the ratio of the average length of true flow paths (microscopic) to the length of the system in the flux direction (macroscopic).

From that definition, it can be noticed that tortuosity depends also on the mechanism of the material transport, not only on the microscopic geometry of the pores. Although tortuosity is dependent on the transport mechanism in the previous definition, it could also be introduced without referring to any specific transport mechanism.

This could be done by taking into account the shortest continuous routes between any two points within the pore space. The main benefit of this definition is that the tortuosity will completely characterize the porous medium itself. However, it seems very natural to use the flux associated with the actual transport system in the concept of tortuosity while taking into account tortuosity in the sense of transport phenomena.

In addition, even without direct reference to the lengths of the transport routes, it is possible to describe tortuosity by taking into account local variations in the microscopic flux direction from the mean flux direction.

3.6.2 Tortuosity of flow in porous media

As discussed before the Darcy's law eq. 2.26 and Kozeny eq. 2.31 where c_0 for cylindrical capillaries is 2. The easiest way to establish tortuosity in the capillary model is to make the capillary tubes inclined in such a manner that a fixed angle θ is formed between the normal of the surface of the material and the axes of the capillary tubes.

In this particular case permeability becomes $k = c_0 \varphi^3 / \tau M^2$ as mentioned before.

where the tortuosity factor $\tau = 1/\cos\theta$ can be given in term of the length of the capillary tube L_e and the medium thickness L as

$$\tau = \frac{L_e}{L} \quad 3.37$$

For the fluid flow in a real porous media, actual tube length can be replaced by the average length of the flow routes of a fluid particle within the sample. To take this average, two possible alternatives may be considered. The first way is to disregard that that a fluid particle may move along the flow paths at different velocities and to average over the actual lengths of the flow paths.

The second way is to average over the lengths of the flow paths of all fluid particles passing through a particular cross section during a given time period. This leads to flux weighted averaging. The first way of averaging is suitable at least for piston-like flows. The second way looks like more natural in the case of fluid flow in porous media.

consider now a solid material has thickness L , has N cylindrical capillary tubes. Assuming that the tubes are straight and have equal radius R , they also have a randomly varying angle between them and the horizontal axis. Thus $\tau_i = L_i/L$.

Next, consider a flow through the capillaries inducing by utilizing a pressure difference Δp across the sample. By solving the Navier-Stokes equation for each capillary tube separately, the average rate through the sample can be determined, with the result

$$q = - \frac{\varphi^3}{2M^2} \frac{\nabla p}{\mu} \frac{\frac{1}{N} \sum_{i=1}^N 1/\tilde{\tau}_i}{\frac{1}{N} \sum_{i=1}^N \tilde{\tau}_i} \quad 3.38$$

This leads to a suggestion of the definition for the tortuosity within this capillary model in the form

$$\tau^2 = \frac{\frac{1}{N} \sum_{i=1}^N 1/\tilde{\tau}_i}{\frac{1}{N} \sum_{i=1}^N \tilde{\tau}_i} \quad 3.39$$

To generalize the previous expression in such a form that is more suitable for real porous media, the sums must be converted into integrals over an arbitrary plane A, perpendicular to the x axis. and the average flow velocity in the i^{th} capillary v_i is independent of i

$$\frac{1}{N} \sum_{i=1}^N \tilde{\tau}_i = \frac{\sum_{i=1}^N \tilde{\tau}_i v_i A_i}{\sum_{i=1}^N v_i A_i} = \frac{\int A \tilde{\tau} v dA}{\int A v dA} \quad 3.40$$

Here, $v=|v(r)|$ is the tangential velocity of the fluid at point r , and $\tilde{\tau} = \tilde{\tau}(r)$ is the ratio of the length of the flow line passing through the point r to the thickness of the sample.

This will lead to the form of the tortuosity that used in this work

$$\tau_v \equiv \frac{\langle |V| \rangle}{\langle v_x \rangle} \quad 3.41$$

3.7 Effective porosity

Porosity (ϕ) is considered as a macroscopic porous medium property and is defined as the ratio of volume of the pore space (V_p) to the bulk volume (V_b) of a porous medium (say, of a rock sample):

$$\phi = V_p/V_b = (V_b - V_s)/V_b \quad 3.42$$

where V_s is the volume of solids within V_b in (2.24) is the total pore space, regardless of either the pores are interconnected or not, this porosity is considered as absolute or total porosity.

However, from the point of view of the fluid flow through the porous medium, only interconnected pores are of interest. Therefore, effective porosity, ϕ_e , has to be introduced as the ratio of the interconnected pore volume, $(V_p)_e$ to the total volume of the medium:

$$\phi_e = \frac{(V_p)_e}{V_b}, \quad (V_p)_e + (V_p)_{ne} = V_p \quad 3.43$$

4 Case studies, methodology and discussion of results

4.1 Case studies

The porous media characterization in this work is done using a set of 2D images binary acquired from thin sections of 3D samples of three different sedimentary rocks.

The first rock used in this work is Berea, this rock is a sandstone rock which is medium-to-fine-grained with ($D_{50} = 23 \mu\text{m}$ Gao and Hu, 2015), this rock is characterized by great difference between the dimension of pore throat and pore body.

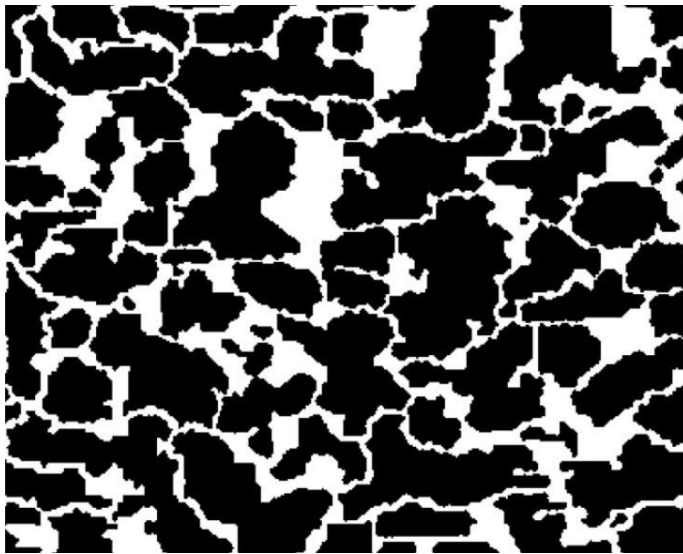


Figure 4.1 2D binary image of Berea sandstone

The second rock sample simulated in this work is Hostun which is homogeneous, and characterized by well-sorted mainly quartz with angular grains ($D_{50} = 300 \mu\text{m}$ Vitorge et al., 2013)

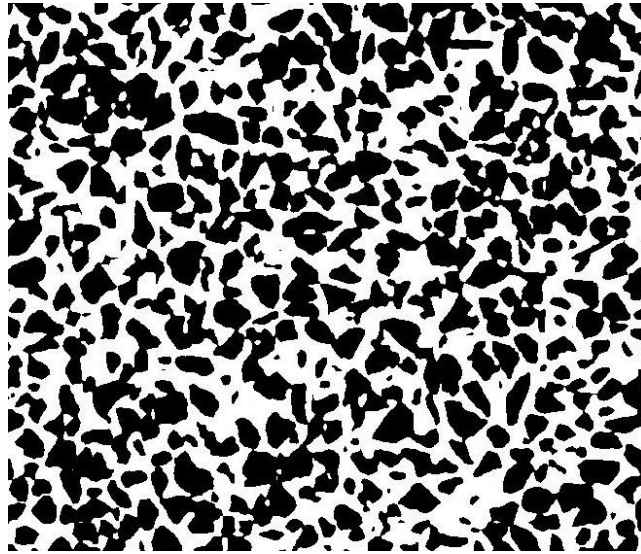


Figure 4.2 2D binary image of Hostun sandstone

The last rock sample used is ooid ($D_{50} = 420 \mu\text{m}$ Andóet al., 2012) which is characterized as a homogeneous rock and characterized by round calcite grains

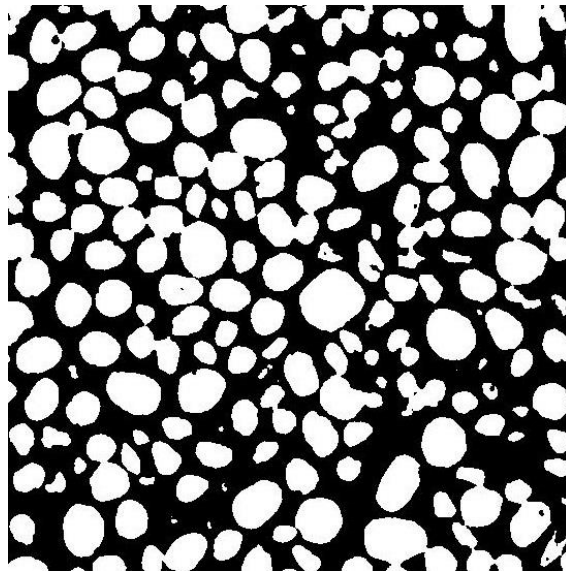


Figure 4.32D binary image of Oodis

The three rock have both high porosity and permeability values make them a potential source of oil and natural gas, consequently in literature they are used as standard rocks for several applications like core analysis, flooding experiment, evaluating the efficiency of EOR (enhanced oil recovery) such as surfactants flooding.

4.2 Methodology

4.2.1 Finite Volume Method (FVM)

The numerical method used in the simulation in this work is the Finite Volume Method (FVM) is considered as one of the numerical techniques that transforms the partial differential equations (PDE) indicating conservation laws over differential volumes into distinct algebraic equations over finite volumes.

In a similar way to the other finite methods (the finite difference or finite element method), the first step in the solution procedures is to discretize the geometric domain into non-overlapping elements or finite volumes. The second step is to transform the partial differential equations into algebraic equations, this done by integrating them over each discrete volume. The third step is solving the algebraic equations system, in order to compute the values of the dependent variable for each of the elements.

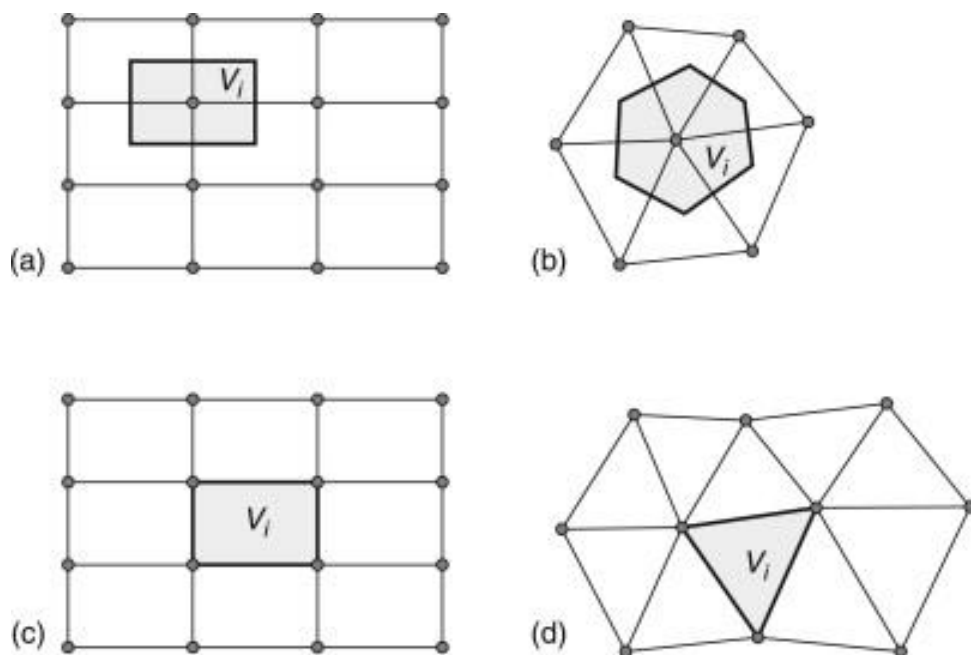


Figure 4.4 Mesh and dual mesh in FVM (a, b) vertex-centered and (c, d) cell-centered. The control volumes are the grey-colored areas

In the finite volume method, a few of the terms in the conservation equations are turned into face fluxes and evaluated at the faces of the finite volume. The FVM is considered strictly conservative Because the flux enters a particular volume is the same as that leaving the neighboring volume. This intrinsic conservation property for the FVM makes it the most appropriate method in CFD¹.

Another important aspect of the FVM is that it can be formulated in the physical space on unstructured polygonal meshes. Finally, using FVM it is easy to apply a range of boundary conditions in a non-intrusive approach, because the unknown variables are estimated at the centroids of the volume elements, not at their boundary faces. Those advantages of the FVM method have made it more suitable for the numerical simulation of a range of applications including fluid flow, heat transfer, mass transfer.

Nowadays the FVM method can deal with all types of complex physics and applications.

4.2.2 OpenFoam

The simulator used in this work is OpenFOAM (which stands for "Open-source Field Operation And Manipulation") is a toolbox written by C++ language, for the development of adapted numerical solvers, and preprocessing and postprocessing utilities for the solution of computational fluid dynamics (CFD).

The first step in the simulation is to create the mesh, particularly a static mesh that its geometry does not change in time. The OpenFOAM meshing utility is called snappyHexMesh which *“is a fully parallel, split hex, mesh generator that guarantees a minimum mesh quality. Controlled using OpenFOAM dictionaries, it is particularly well suited to batch driven operation. It starts from any pure hex mesh (structured or unstructured) reads geometry in triangulated formats, e.g. in stl, obj, vtk. No limit on the number of input surfaces”* OpenFOAM user guide.

¹ Computational Fluid Dynamics (CFD) is a powerful numerical simulation tool, however the initial motivation of developing CFD was provided for particularly the aerospace industry and some sections within the aeronautic, nowadays CFD is considered as an essential tool in a range of other design intensive industries such as the nuclear, power generation, chemical, automotive, and marine industries.

The snappyHexMesh tool can create a 3-D mesh around a body that is defined by a surface mesh, such as Stereolithography (.stl) file. The rock images used in this work were .jpg files, so they had to be converted to .stl files to be used in snappyHexMesh, this was done using a MATLAB code.

Fundamentally, snappyHexMesh identifies the intersections between the input body surface (figure 3.5), and a created background mesh (figure 3.6) that comprises only hexahedral cells and has external geometry as the system geometry, this background mesh is created using another utility called blockMesh.

The number of cells or the background mesh dimensions is designed to be large to cover the small pore throats in the sample, in this work the number of cells in x-direction is set to be 2000 cells while in y-direction is calculated from the aspect ratio between the original image dimensions. After that it eliminates the cells occupied by the body (figure 3.7).

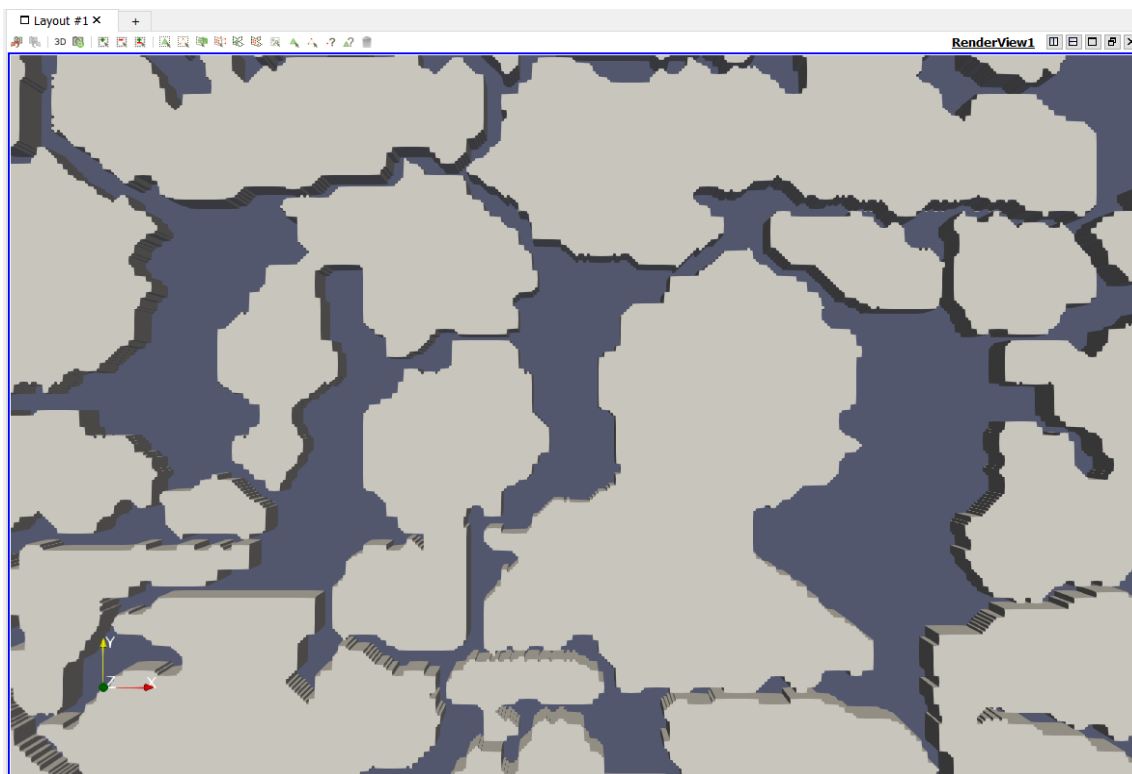


Figure 4.5 .stl file created using MATLAB for the original .jpg file for the rock image

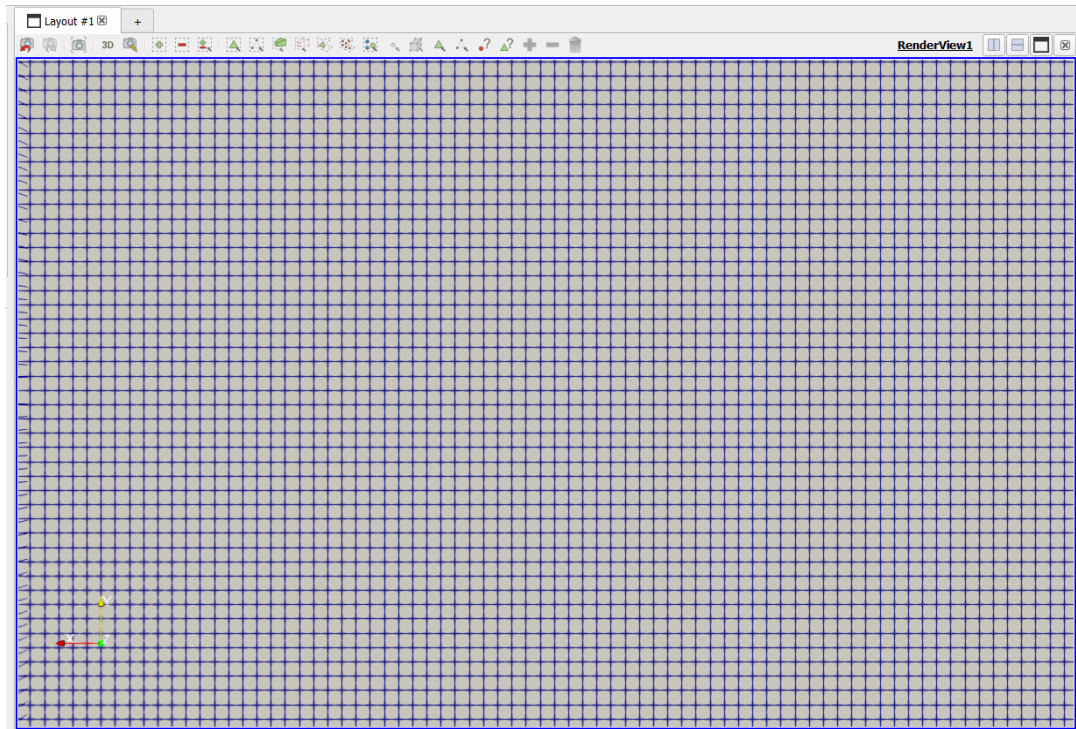


Figure 4.6 a created background mesh done by blockMesh utility in OpenFOAM

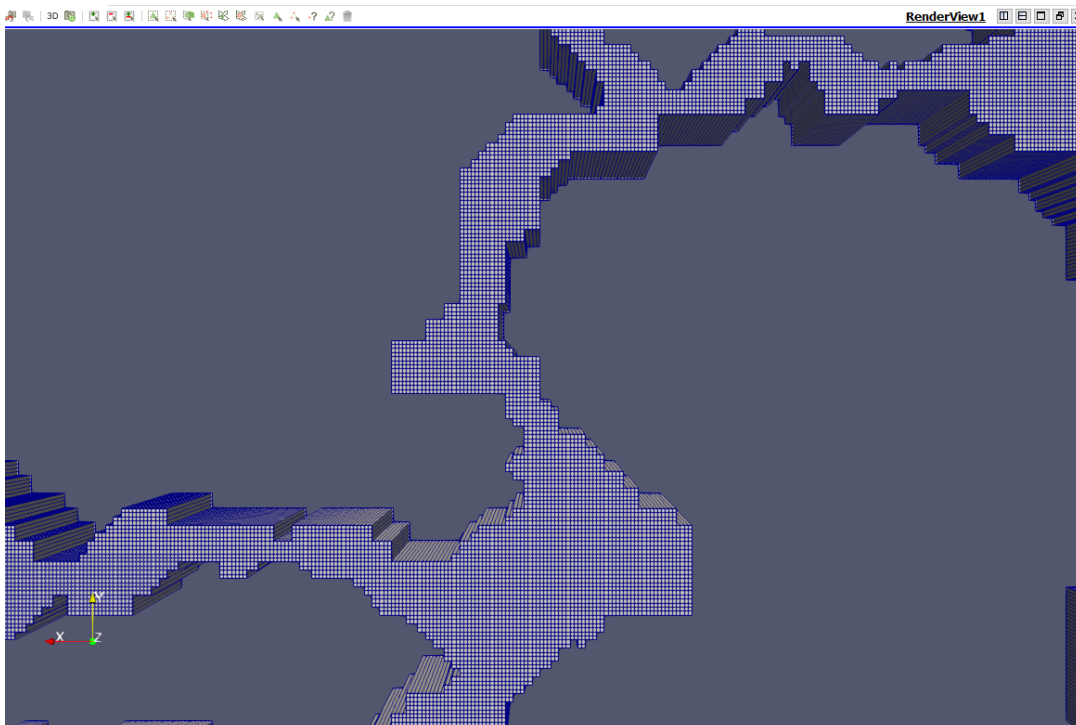


Figure 4.7 the final mesh created by snappyHexMesh utility in the pore space only

It is important to mention here the mesh creating technique and the application of the concept of effective porosity which has been discussed in section (2.7)

As mentioned before, the only of interest here is the interconnected pore voids, however in the case of Huston rock image in this work, there is a significant pore voids part which is completely isolated from the other pores, the snappyHexMesh utility will deal with it as a solid phase or particularly non fluid flow probable paths.

As seen in figure (3.8) the highlighted pore voids area is completely isolated from the other pores, and in figure (3.9) there is no mesh gridding in that area

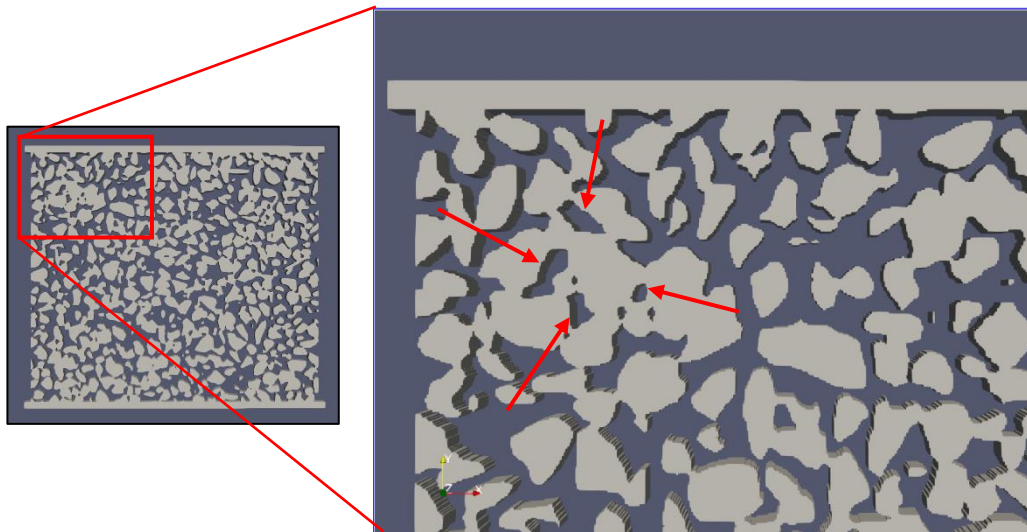


Figure 4.8 A zoom on the non-interconnected pore space in Huston rock image

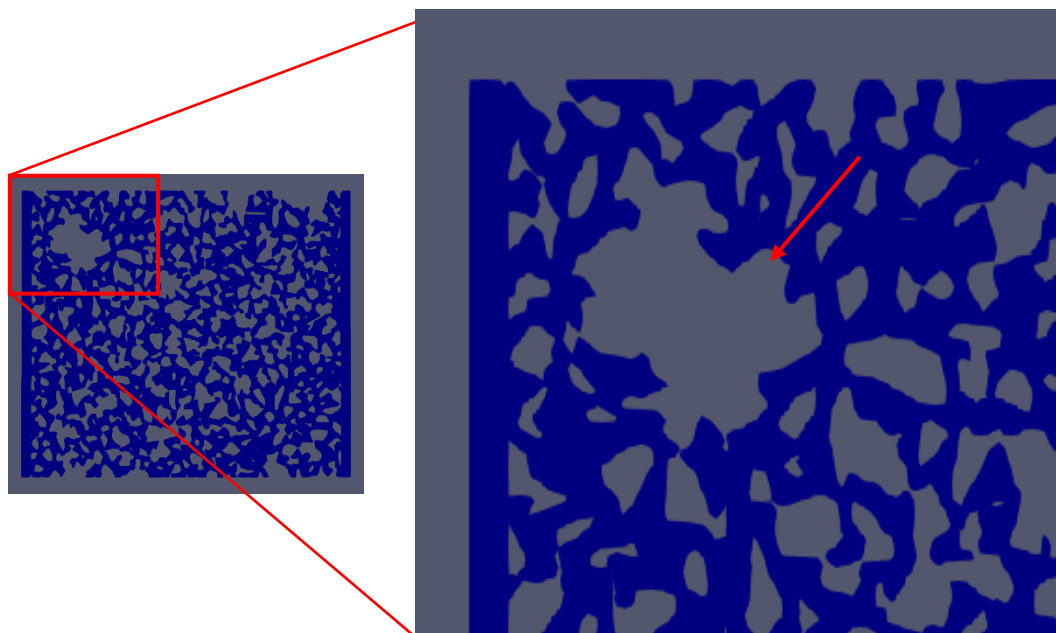


Figure 4.9 The resulted mesh showing the effect of the effective porosity

After creating the mesh inside the pore space, now it is the time to set the boundary conditions, The identification of the isothermal, 2-D and incompressible single phase flow in the pore space is obtained by solving Navier-Stokes equations. Consequently, the boundary conditions are necessary for the following parameters: velocity components in x-direction (u_1) and y-directions (u_2), pressure (p).

In this work the horizontal direction is considered to be the main flow path, hence it is possible to neglect the gravity effect on the flow. For the fluid in contact with the solid walls of the pores the non-slip condition is considered as a boundary condition. The inlet and outlet boundary conditions are set as fixed values with a 100 pa/m gradient, the velocity is calculated depending on the pressure as a keyword `pressureInletVelocity`.

The following step is to run the solver, in this work, SimpleFoam is the used solver and it is defined as a steady-state solver for incompressible, turbulent flow, using the SIMPLE (Semi-Implicit Method for Pressure Linked Equations) algorithm.

The strategy of SimpleFoam solution is that it follows a separated solution strategy. This strategy means that the equations for each parameter describing the system is solved in sequence and the solution of the preceding equations is inserted in the following equation. Thus, the non-linearity occurring in the momentum equation is resolved by estimating it from the velocity and pressure values of the previous iteration.

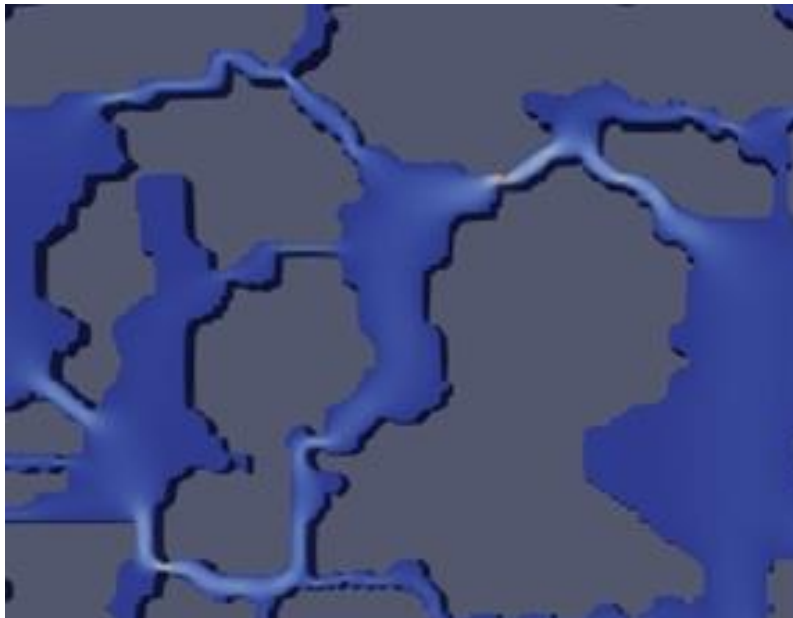


Figure 4.10 velocity in x-direction results using simpleFoam solver

The OpenFOAM output is the velocity in x-direction and y-direction and the pressure, as mentioned in the objective the purpose of this work is to characterize the porous media, and this will be done by calculating permeability and tortuosity.

One more step is required to calculate both permeability and tortuosity from the simulation results. A MATLAB code has been written to calculate them.

```

1 -   clc; clear all; close all;
2 -   %%read excel file
3 -   t = xlsread('Berea-1st_run-3D0.csv'); %read csv file as an excel file
4 -   first=t(1:length(t));           %read first column Velocity X-dir...vector
5 -   second=t(length(t)+1:length(t)*2); %read second column Velocity Y-dir..vector
6 -   third=t(length(t)*2+1:length(t)*3); %read third column Velocity Z-dir...vector
7 -   forth=t(length(t)*3+1:length(t)*4); %read forth column pressure...vector
8
9 -   %%.....%%
10
11  %%Tortuosity Calculatoins
12 -   averagex=mean(first);           %velocity in X-dir.....scalar
13 -   m=first.^2;                    %square of velocity_x_dir
14 -   n=second.^2;                   %square of velocity_y_dir
15 -   l=m+n;
16
17 -   VelocityMagnitude=sqrt(l); %Velocity=sqrt{(vel-X)^2+(vel-Y)^2}....vector
18 -   Velocity=mean(VelocityMagnitude);%Velocity....scalar
19 -   Tortuosity=Velocity/averagex;
20
21  %%.....%%
22
23  %%Permeability Calculatoins
24  |
25 -   Cell_no = 1800*1354*8;          % number of cells
26 -   Darcy_Vel = sum(first)/Cell_no; % Velocity
27 -   %Darcy Velocity is the average of velocity values for all cells {rock cells
28 -   %and pore cells}
29 -   vis = 0.0005;                  % %viscosity "nu"....pa.s
30 -   %p1 = 0.187;                   % inlet pressure....pa
31 -   p1= max(forth)*1050;% inlet pressure....pa
32 -   p2 = 0 ;                       % outlet ressure....pa
33 -   x = 0.00187;                   % length.....m
34 -   k = (Darcy_Vel * vis * x)*1e15/(p1-p2); %md

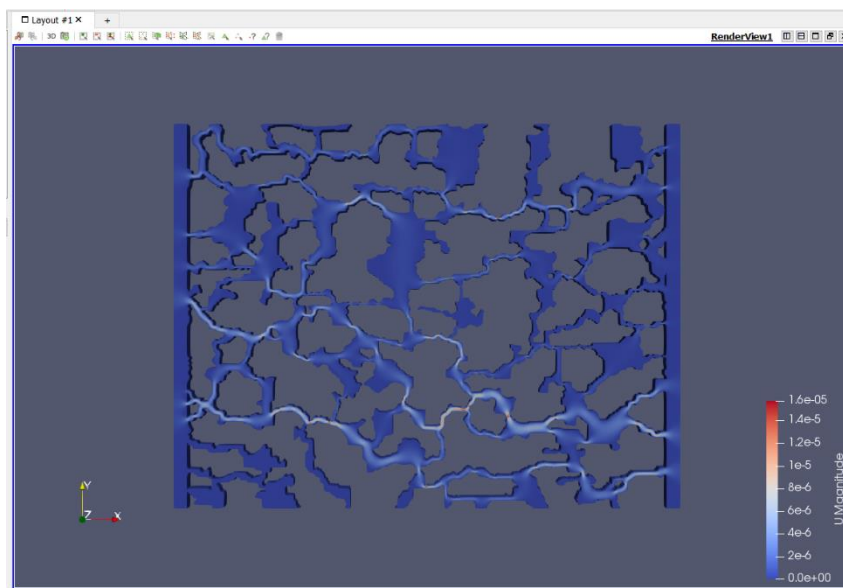
```

Figure 4.11 the MATLAB code used in permeability and tortuosity calculations

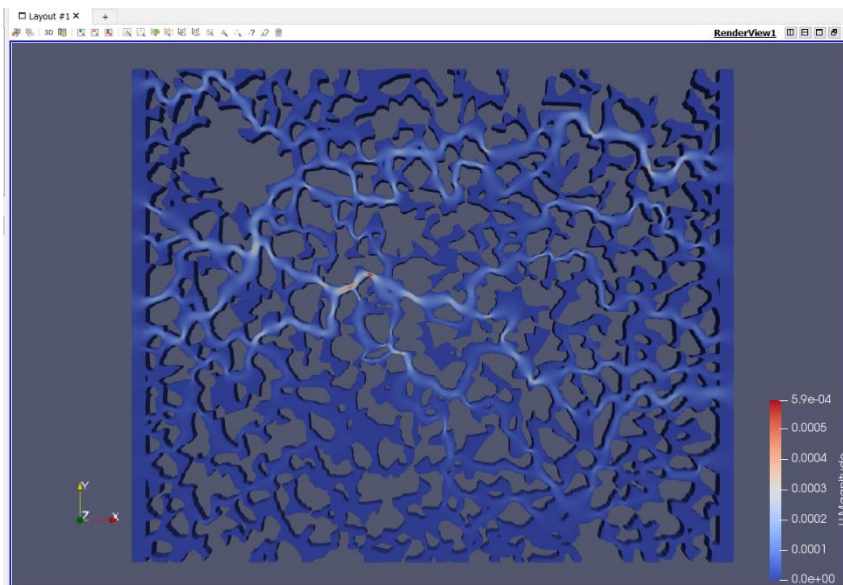
4.3 Results and discussion

4.3.1 Part 1: porous media characterization

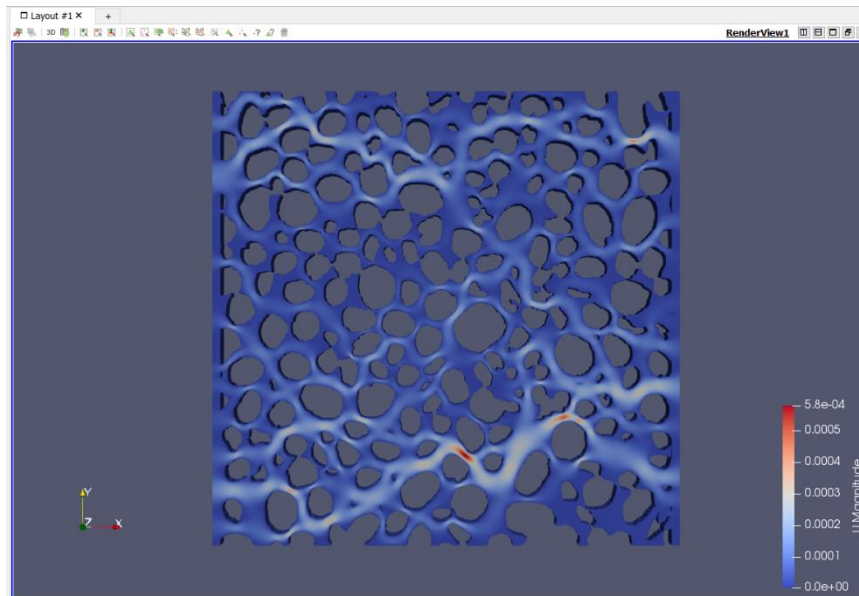
The first part of this work is the simulation of the porous media to characterize it, the following figures is the velocity in x-direction values calculated by OpenFOAM for the three rock images.



(a)

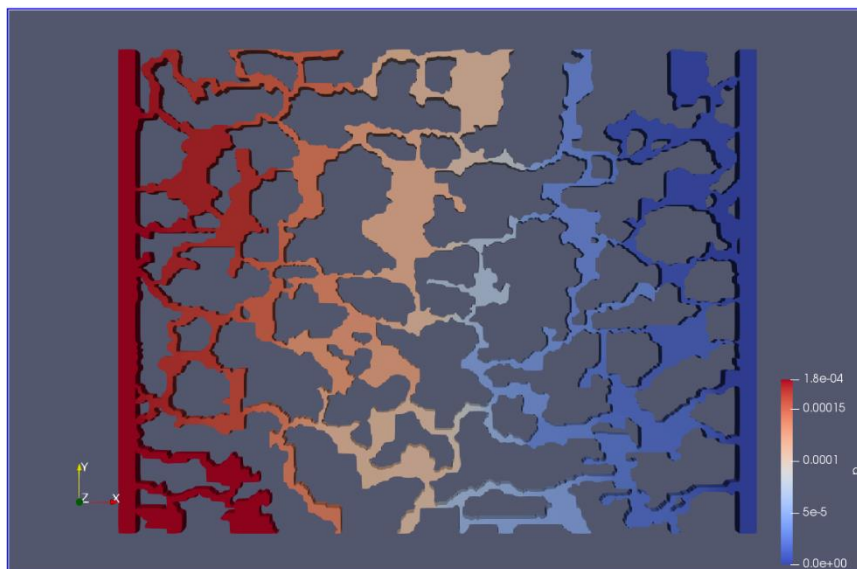


(b)

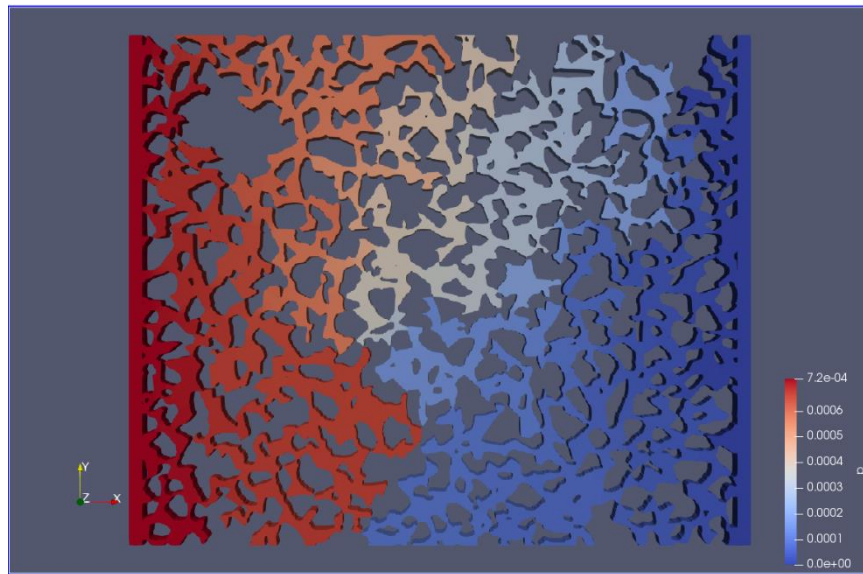


(c)

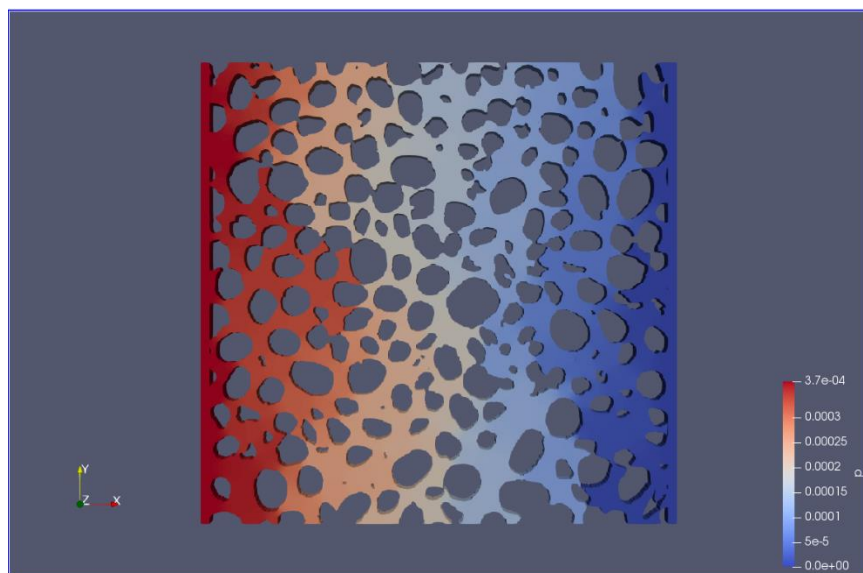
Figure 4.12 X-Direction velocity values resulting from the simulation of the three rock samples (a) Berea, (b) Hostun and (c) Oodis



(a)



(b)



(c)

Figure 4.13 Pressure values resulting from the simulation of the three rock samples (a) Berea, (b) Hostun and (c) Oodis

Rock Image Name	No. of cells	Velocity in X-direction	Tortuosity	Permeability
		m/s	ratio	Darcy
Berea	2437200	1.6555E-07	1.5670	0.825
Hostun	4626000	1.9862E-04	1.2882	9.9117
Oodis	4000000	1.4050E-05	1.3712	6.9428

Table 1 The results of the simulation used for porous media characterization the first part of this work

As shown in the previous table we can notice the range of the values for permeability and tortuosity, we can establish a relationship between the two parameters, that it can be easily noticed that for the more tortuous rock the less permeable.

4.3.2 Part 2: Sensitivity analysis of the effect of the thickness of the 3D model on the calculated permeability using 2D+ model

In the second part of this work, a 3D model generated from the 2D image of Berea adding a constant thickness (called 2D+ model) was considered. The purpose is to investigate the influence of the distance between the top and the bottom walls (thickness) on the permeability value.

To do that three different thicknesses were used based on the minimum pore size, the minimum pore size is obviously a pore throat and is equal to 4.1556E-6 m. The three thicknesses were defined as three, six and twelve times the minimum pore size.

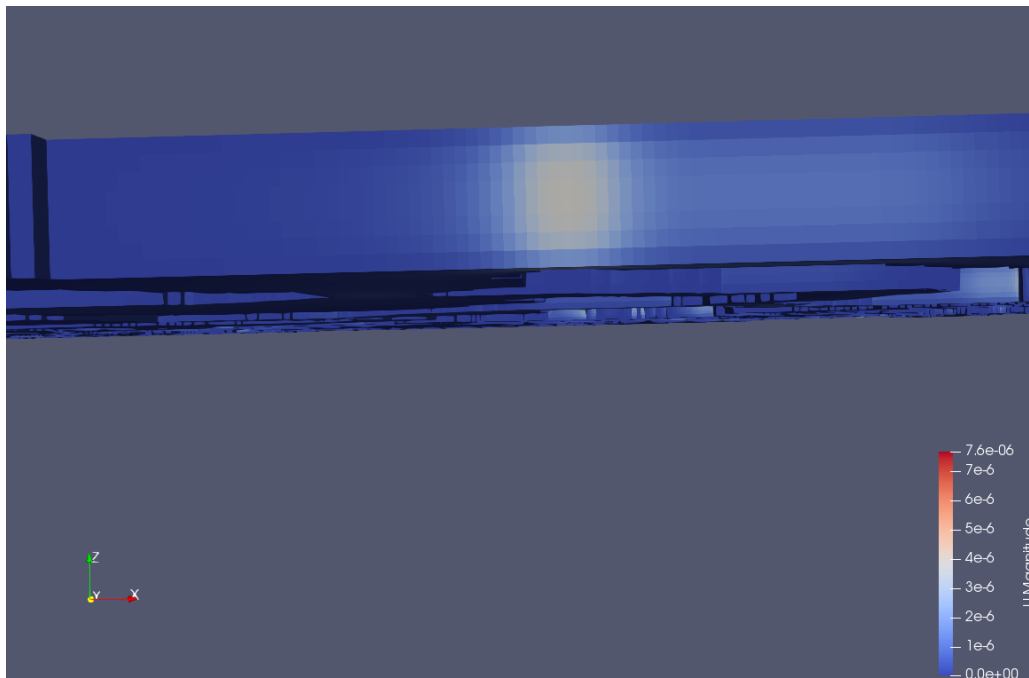


Figure 4.14 The velocity values in Z-direction for the 2D+ model showing a gradually change in the values

The results showed that increasing the thickness of the 3D model, the permeability increases, approaching the permeability of the 2D model evaluated in the first part of the study; in fact, when the distance between top and bottom becomes bigger, the influence of the drag force on the fluid becomes smaller. Further investigation is recommended to examine the proper thickness of the 3D model that should be used to have the consistency of the permeability value.

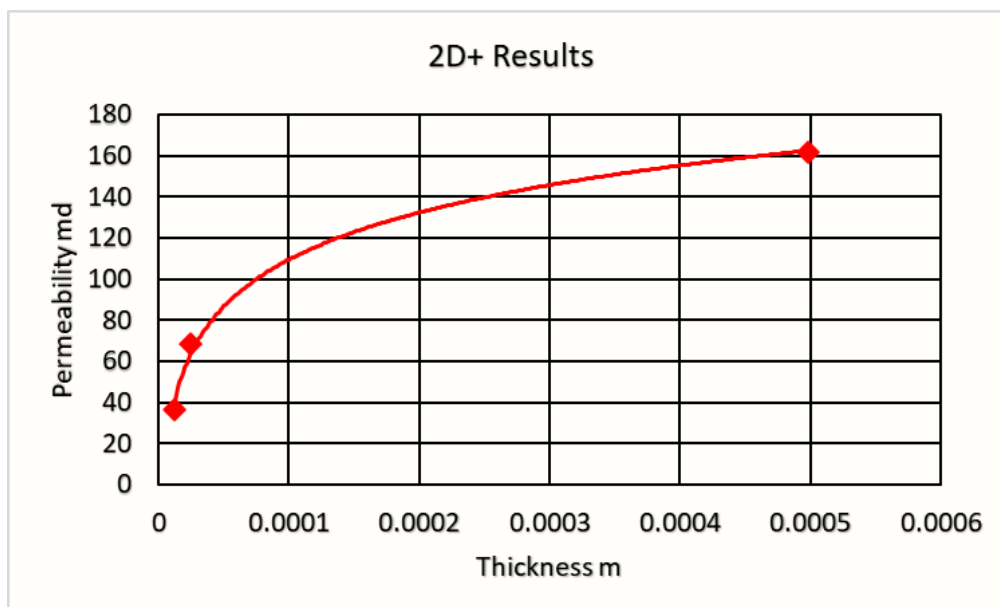


Figure 4.15 2D+ results of the sensitivity analysis of the thickness influence on the permeability values

5 Conclusion

In this thesis, single-phase flow simulations in porous media at the pore scale has been done using direct numerical simulation (DNS), which consists in solving numerically Navier-Stokes equations (NSEs) over the entire domain of interest.

In this study, the OpenFOAM code, which is based on the Finite Volume Method (FVM), was used for solving the problem. A preliminary literature review found this method to be adequate for the simulation of fluid flow in complex geometries such as porous media.

The simulations have been done on 2D binary images of three different sedimentary rocks: Berea sand ($D_{50} = 23 \mu\text{m}$), Hostun sand ($D_{50} = 300 \mu\text{m}$) and Caicos ooids ($D_{50} = 420 \mu\text{m}$).

The thesis is mainly divided into two parts. The purpose of the first part of this work is to characterize the porous media by estimating the permeability (k) and tortuosity (τ), using the velocity field obtained by direct numerical simulation.

The porous media characterization at the pore scale is done to investigate the influence of the microscale parameter tortuosity on the macroscale parameter permeability: the permeability is inversely related to the tortuosity, as expected.

In the second part of the thesis, a constant thickness 3D model based on the 2D image of Berea was considered (called 2D+ model), with purpose to investigate the influence of the top and bottom wall on the permeability value. Three different thicknesses, equal to three, six and twelve times the minimum pore size, were investigated.

The results showed that increasing the thickness of the 3D model, the permeability increases, approaching the permeability of the 2D model evaluated in the first part of the study; in fact, when the distance between top and bottom becomes bigger, the influence of the drag force on the fluid becomes smaller.

Further investigation is recommended to examine the proper thickness of the 3D model that should be used to have the consistency of the permeability value.

6 References

1. A. E. Scheidegger, Macmillan, The Physics of Flow Through Porous Media, New York, 1957.
2. A. Koponen, M. Kataja, and J. Timonen, Tortuous flow in porous media Department of Physics, University of Jyväskylä, PL 35, SF-40351 Jyväskylä, Finland, 1996.
3. Ana Žgaljić Keko, Modelling, Analysis and Numerical Simulations of Immiscible compressible Two-phase Fluid Flow in Heterogeneous Porous Media.
4. Brett William Gunnink, Determination of the pore structure of porous materials using electrical conductance, Iowa State University, 1987.
5. Bruno Braga, Direct Numerical Simulations of Two-Phase Flow in Porous Media: A Sensitivity Analysis of Relative Permeabilities, Tesi di Laurea, POLITECNICO DI MILANO, 2017.
6. Cyprien Soullaine, SIMULATION TECHNIQUES TO MODEL FLOW AND TRANSPORT AT THE PORESCALE, 2018.
7. Dario Viberti, Costanzo Peter, Eloisa Salina Borello, Filippo Panini, Pore structure characterization through pathfinding and Lattice Boltzmann simulation.
8. Dullien Article, Characterization Of PorousMedia, 1991.
9. F. Moukalled, L. Mangani, M. Darwish, The Finite Volume Method in Computational Fluid Dynamics, An Advanced Introduction with OpenFOAM® and Matlab®.

References

10. George, The Effect of the Internal Friction of Fluids on the Motion of Pendulums. Transactions of the Cambridge Philosophical Society Stokes, (1851).
11. H K Versteeg and W Malalasekera, An Introduction to Computational Fluid Dynamics THE FINITE VOLUME METHOD.
12. Hilmi S. Salem, Application of the Kozeny-Carman Equation to Permeability Determination for a Glacial Outwash Aquifer, Using Grain-size Analysis, 2001.
13. Jack Dvorkin, KOZENY-CARMAN EQUATION REVISITED, 2009.
14. Lawrence M. Anovitz, Characterization and Analysis of Porosity and Pore Structures, Chemical Sciences Division Oak Ridge National Laboratory Oak Ridge, Tennessee, USA Reviews in Mineralogy & Geochemistry Vol. 80 pp. 61-164, 2015.
15. M. R. J. WYLLIE² AND M. B. SPANGLER, APPLICATION OF ELECTRICAL RESISTIVITY MEASUREMENTS TO PROBLEM OF FLUID FLOW IN POROUS MEDIA Pittsburgh, Pennsylvania (1952).
16. Martin J. Blunt, Multiphase flow in permeable media, A Pore-Scale Perspective, Imperial College London, 2017.
17. Michael Clennell Tortuosity: A guide through the maze, Geological Society London Special Publications, January 1997.
18. Molly S. Costanza-Robinson, Benjamin D. Estabrook, and David F. Fouhey, Representative elementary volume estimation for porosity, moisture saturation, and air-water interfacial areas in unsaturated porous media: Data quality implications Received 14 June 2010; revised 5 May 2011; accepted 23 May 2011; published 8 July 2011.
19. White Frank, Viscous Fluid Flow. 3rd Edition. McGraw-Hill Mechanical Engineering, (1991).
20. OpenFOAM user guide.

References

21. R. Byron Bird, Warren E. Stewart, Edwin N. Lightfoot., Transport phenomena, 1924.
22. Zhilin Li, Zhonghua Qiao and Tao Tang, Numerical solution of differential equations, Introduction to finite difference and finite element methods.